Escuela Superior Politécnica del Litoral

Facultad de Ingeniería en Ciencias de la Tierra

Geoeléctrica y sísmica de refracción para zonificación de áreas inestables en el campamento Guarumales

Previo la obtención del Título de:

Magíster en Geotecnia

Modalidad: Artículos Profesionales de Alto Nivel

Presentado por:
Edgar Esteban Molina Torres y Roberto Isaac Avalos Sánchez

Guayaquil - Ecuador
Año: 2026

Declaración Expresa

Nosotros, Edgar Esteban Molina Torres y Roberto Isaac Avalos Sánchez, acordamos y reconocemos que:

La titularidad de los derechos patrimoniales de autor (derechos de autor) del proyecto de graduación corresponderá al autor o autores, sin perjuicio de lo cual la ESPOL recibe en este acto una licencia gratuita de plazo indefinido para el uso no comercial y comercial de la obra con facultad de sublicenciar, incluyendo la autorización para su divulgación, así como para la creación y uso de obras derivadas. En el caso de usos comerciales se respetará el porcentaje de participación en beneficios que corresponda a favor del autor o autores.

La titularidad total y exclusiva sobre los derechos patrimoniales de patente de invención, modelo de utilidad, diseño industrial, secreto industrial, software o información no divulgada que corresponda o pueda corresponder respecto de cualquier investigación, desarrollo tecnológico o invención realizada por nosotros durante el desarrollo del proyecto de graduación, pertenecerán de forma total, exclusiva e indivisible a la ESPOL, sin perjuicio del porcentaje que nos corresponda de los beneficios económicos que la ESPOL reciba por la explotación de nuestra innovación, de ser el caso.

En los casos donde la Oficina de Transferencia de Resultados de Investigación (OTRI) de la ESPOL comunique a los autores que existe una innovación potencialmente patentable sobre los resultados del proyecto de graduación, no se realizará publicación o divulgación alguna, sin la autorización expresa y previa de la ESPOL.

Guayaquil, 14 de abril de 2026

Edgar Esteban Molina Torres

Roberto Isaac Avalos Sánchez

Evaluadores

Firmado electrónicamente por:
DAVIDE BESENZON VENEGAS
Validar únicamente con FirmaEC

Ph. D. Davide Besenzon Venegas

Profesor de Materia

Firmado electrónicamente por:
SAMANTHA TAMARA JIMENEZ OYOLA
Validar únicamente con FirmaEC

Ph. D. Samantha Jiménez Oyola

Profesor de Materia

Firmado electrónicamente por:
PAUL CESAR CARRION MERO
Validar únicamente con FirmaEC

Ph. D. Paúl Carrión Mero

Tutor de proyecto

Resumen

Los movimientos en masa son eventos geológicos que implican el desplazamiento de suelo, ocasionando tanto daños materiales como pérdidas de vidas humanas. La localización de centrales hidroeléctricas incrementa la susceptibilidad a fenómenos de movimientos en masa. El Proyecto Paute Integral (Azuay—Ecuador) está conformado por tres presas que abastecen aproximadamente el 35 % de la demanda energética del país. El campamento "Guarumales" se localiza en una zona de macrodeslizamiento con presencia de aguas subterráneas, lo que representa un riesgo para la infraestructura operativa y administrativa de una de sus principales plantas de producción.

La presente investigación tiene como objetivo generar un mapa de susceptibilidad a deslizamientos del campamento mediante la correlación de métodos geofísicos (Tomografía de Resistividad Eléctrica y Sondeos Eléctricos Verticales) para identificar zonas críticas. Para este propósito se desarrollaron cuatro procesos: (i) caracterización de los factores de inestabilidad a partir de información temática base, (ii) campaña de exploración geofísica, (iii) cartografía en un entorno SIG y (iv) zonificación de la estabilidad.

La integración de estas variables permitió delimitar áreas con alta susceptibilidad, caracterizadas por bajos valores de resistividad, materiales poco competentes y saturación hídrica en pendientes pronunciadas. Asimismo, se identificó inestabilidad asociada a procesos de erosión y socavación en las márgenes de los cauces cercanos al campamento y en zonas de recarga, donde la capa saturada presenta resistividades bajas (<75 Ω·m). En contraste, las áreas con altos valores de resistividad (>5000 Ω·m) y cobertura forestal evidenciaron una mayor estabilidad.

Los resultados de esta zonificación constituyen un insumo fundamental para la planificación territorial y la definición de medidas de mitigación basadas en evaluaciones in situ, contribuyendo a la reducción del riesgo en proyectos hidroeléctricos emplazados en entornos geológicos complejos.

Palabras clave: Tomografía de resistividad eléctrica, sondeos eléctricos verticales, fenómenos de remoción en masa, estabilidad de taludes, análisis de susceptibilidad, cartografía.

Abstract

Mass movements are geological events that involve the displacement of soil, causing both material damage and loss of human life. The location of hydroelectric plants increases susceptibility to mass movement phenomena. The Paute Integral Project (Azuay—Ecuador) consists of three dams that supply approximately 35% of the country's energy demand. The "Guarumales" camp is in a macro-landslide zone with groundwater, posing a risk to the operational and administrative infrastructure of one of its main production plants.

This research aims to generate a landslide susceptibility map of the camp by correlating geophysical methods (Electrical Resistivity Tomography and Vertical Electrical Soundings) to identify critical zones. For this purpose, four processes were carried out: (i) Characterization of instability factors using baseline thematic information, (ii) geophysical exploration campaign, (iii) GIS mapping, and (iv) stability mapping.

The integration of these variables enabled delineation of areas with high susceptibility, characterized by low resistivity values, weak materials, and water saturation on steep slopes. Likewise, instability associated with erosion and undercutting was identified on stream banks near the camp and in recharge areas where the saturated layer is characterized by low resistivities (<75 Ω·m). In contrast, areas with high resistivity values (>5000 Ω·m) and forest cover exhibited greater stability.

The results of this zonation provide a fundamental input for territorial planning and defining mitigation measures based on in situ evaluations, contributing to risk reduction in hydroelectric projects located in geologically complex environments.

Keywords: Electrical resistivity tomography, Vertical electrical soundings, mass removal phenomena, slope stability, susceptibility analysis, mapping.

Índice general

Abreviaturas

- ABEM: ABEM Instrumentos Geofísicos
- AIMS: Análisis Integrado Multicriterio de Susceptibilidad
- AMSS: Análisis Multicriterio de Susceptibilidad a Deslizamientos
- CELEC EP: Corporación Eléctrica del Ecuador, Empresa Pública
- DEM: Modelo Digital de Elevación (Digital Elevation Model)
- ERT: Tomografía de Resistividad Eléctrica (Electrical Resistivity Tomography)
- ESRI: Environmental Systems Research Institute
- FMR: Factor de Material Rocoso
- FR: Factor de Riesgo
- GIS: Sistema de Información Geográfica (Geographic Information System)
- HVSR: Relación Espectral Horizontal-Vertical (Horizontal to Vertical Spectral Ratio)
- IDW: Inversa de la Distancia Ponderada (Inverse Distance Weighting)
- IIGE: Instituto de Investigación Geológico y Energético
- INAMHI: Instituto Nacional de Meteorología e Hidrología
- LS: Factor Longitud-Pendiente (Length–Slope Factor)
- MAGAP: Ministerio de Agricultura, Ganadería, Acuacultura y Pesca
- MRP: Modelo de Riesgo Potencial
- MTOP: Ministerio de Transporte y Obras Públicas
- MW: Megavatio
- PI: Paute Integral
- PP: Punto de Prospección

- PRECUPA: Proyecto Hidroeléctrico Paute Integral
- RF: Factor de Recarga
- SUR: Superficie de Ruptura
- VES: Sondeo Eléctrico Vertical (Vertical Electrical Sounding)
- VGF: Factor de Variación Geológica

Simbología

- Ω·m : Ohmnio Metro

Índice de figuras

Índice de tablas

Chapter 1

1.1 Introduction

Mass movements are among the most destructive natural hazards, causing significant damage to infrastructure and posing a serious threat to human life [1]. These natural processes, characterized by the downslope displacement of soil and rock masses, are common in regions where topographic, geological, meteorological, and hydrological conditions interact to create inherently unstable environments [2]. These unstable conditions often coincide with areas developed for hydropower generation due to their high hydraulic potential [3].

In 2010, governments of several Andean Amazonian countries —such as Peru, Colombia, Brazil, and Ecuador—emphasized investment in hydropower as a core component of medium and long-term plans to meet future energy demand [4]. This emphasis stems from the fact that increasing hydropower generation contributes to achieving the Sustainable Development Goals (SDGs), which, in the international context, promote economic and energy integration between developing and developed countries while reducing economic vulnerability by decreasing dependence on fossil fuels [5].

Currently, Ecuador has 15 hydropower plants, accounting for 72.79% of the country's total installed generation capacity [6], with an effective installed capacity of 6,855.07 MW [7].

Among the eight business units of the Corporación Eléctrica del Ecuador (CELEC EP) that operate hydropower facilities, CELEC SUR stands out as the unit with the highest hydropower production capacity nationwide, reaching 2,001.9 MW. Of this output, 86.51% corresponds to the Paute Integral Complex, which comprises the Paute, Mazar, and Molino projects [6].

The projects mentioned above are in Azuay Province, along the Paute–Guarumales–Méndez roadway, which corresponds to a section of the E-40 highway (see Figure 1).

Hydropower plants are commonly located in mountainous, steep-slope regions where hydrological conditions provide high hydraulic potential; however, these same conditions often coincide with areas prone to landslides due to the presence of materials with low geomechanical strength, residual soils, fractured rock masses, and intense precipitation [8]. This is the case of the Paute integral hydropower complex (CELEC EP), which, as of 2020, has recorded twenty-one mass movement phenomena (MMPs), including the Guarumales landslide [9].

In the areas surrounding the Paute Integral Hydropower Complex, landslides have been identified that have damaged damage to road infrastructure, resulting in accessibility issues to the complex's central operational facility the "Guarumales" camp. In this area, landslides have occurred that have completely disrupted the roadway; a representative example took place in June 2020 at the Jurupis stream (Amaluza Parish), where an approximately 80 m section of the road failed, necessitating a realignment of the roadway axis and the construction of a new bridge [10]

A similar event occurred in 2002 at the Bomboiza 2 Bridge (Bomboiza Stream), where a 600 m long mass movement completely disrupted the roadway [11].

Within this context, the integrity of the Paute Integral Hydropower Complex is critical to national energy production; however, over the past 23 years, several soil movement events have occurred in areas adjacent to the hydropower facilities, including access roads and operational camps. These events have raised significant concern among authorities, to the extent that in 2020 the E-40 highway was declared under a state of emergency, and a cooperation agreement was signed between the Ministry of Transport and Public Works (MTOP) and CELEC to carry out studies along the Paute–Guarumales–Méndez roadway, Amaluza sector [12].

The assessment of the Guarumales landslide led CELEC EP to implement a range of investigation techniques, including geodetic monitoring, the installation of piezometers and rain

gauges, flow measurements in drainage systems, and geotechnical drilling campaigns. These investigations determined that the Guarumales landslide is deep-seated and exhibits slow-moving behavior [8]. Furthermore, through empirical correlation of geophysical methods —Vertical Electrical Soundings (VES) and H/V spectral ratio analysis— it was established that the landslide corresponds to a translational mechanism associated with thick colluvial deposits exceeding 55 m in thickness [13]. These deposits are permeable and poorly saturated, where local infiltration processes play a significant role in the landslide's evolution [8].

Electrical Resistivity Tomography (ERT) has been applied in geophysical exploration campaigns to delineate geoelectrical units by correlating resistivity profiles with local geological conditions [14], [15]. In the 2023 landslide in Alausí, ERT surveys enabled distinguishing altered soil layers, structural systems, and saturation levels [16].

Preventive management of mass movement phenomena (MMPs) requires identifying areas most prone to these natural processes; therefore, mass movement zoning enables a spatially estimating zones that require intervention and monitoring [17], [18]. Zoning models have proven to be effective tools for risk management in urban settlements [19], [20]. Furthermore, the integration of multicriteria analysis in such studies has been used to correlate weighting values with safety factors derived from limit equilibrium methods, as demonstrated in the La Cria community, Azuay Province in Ecuador [21].

Similarly, several authors emphasize that adequate characterization of abiotic elements—such as lithology, geomorphology, soils, and geodynamic processes—is essential for understanding ground stability and for planning territorial management actions [22].

Based on this context, the following research questions arise: (i) How can unstable areas be delineated through the application of geophysical methods in the Guarumales camp? and (ii)

How does geoelectrical surveying contribute to the development of an instability zoning map that enables the assessment of the geotechnical safety of existing infrastructure?

To strengthen the control measures applied at the camp, this study aims to generate a slope stability zoning map by correlating geophysical methods —Electrical Resistivity Tomography (ERT) and Vertical Electrical Soundings (VES)— to identify critical areas requiring complementary investigations.

Figure 1

Location map of the Paute Integral Hydropower Complex (CELEC EP) and the Guarumales Camp

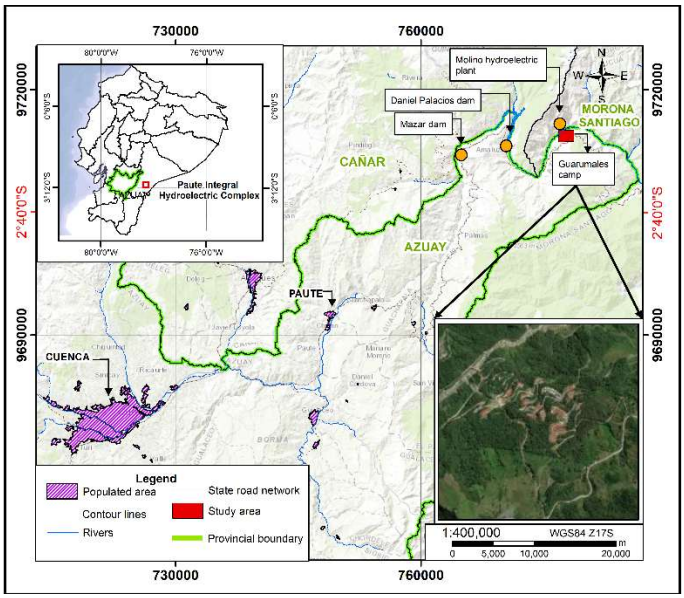

Chapter 2

2.1 Materials and Methods

Mass movement zoning methods consider multiple factors to estimate susceptibility to these natural processes. Such approaches integrate semi-quantitative assessments that weight conditioning and triggering factors [23]. Likewise, these analyses incorporate site knowledge criteria by selecting relevant factors, which are assigning them ranks and weights based on their relative importance [24]. This framework is complemented by surface-based geophysical measurements, including electrical resistivity, to zone by degree of instability and define priority areas for intervention.

The methodological approach was divided into four phases: (1) characterization of instability factors based on baseline thematic information, (2) geophysical exploration campaign, (3) GIS-based mapping, and (4) zoning of unstable areas (Figure 2).

Figure 2

Outline of the methodological process for zoning unstable areas

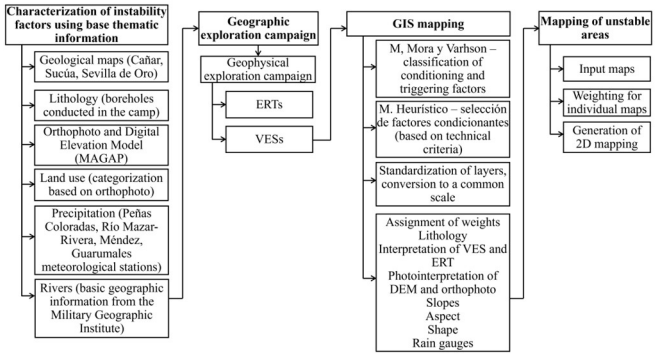

2.1.1 Phase I: Characterization of instability factors based on baseline thematic information

Preliminary and essential information for mass movement zoning was analyzed and compiled, including the Cañar and Sucúa geological map sheets at a 1:100,000 scale from the Geological and Energy Research Institute (IIGE); the geological map of the Sevilla de Oro canton at a 1:25,000 scale from the Natural Disaster Prevention Project in the Paute Basin (PRECUPA); borehole records from the Guarumales camp conducted in November 2016; a Digital Elevation Model (DEM) and 1:5,000-scale orthophotography from the Ministry of Agriculture and Livestock (MAGAP); historical data from the Peñas Coloradas, Río Mazar–Rivera, and Méndez meteorological stations of the National Institute of Meteorology and Hydrology of Ecuador (INAMHI); and data from the Guarumales station operated by the CELEC SUR Hydropower Plant.

2.1.2 Phase II: Geophysical exploration campaign

The layout and positioning of the geophysical survey lines were determined through site inspections of areas within the Guarumales camp that showed evidence of instability, including subsidence, undercutting, pavement loss, material detachment, erosion, and failures in retaining structures. During the geophysical exploration campaign, electrical methods were applied (VES and ERT) using an ABEM Terrameter LS-2 system.

The geophysical campaign included eight Vertical Electrical Soundings (VES) with investigation depths ranging from 98 to 145 m, using a Schlumberger array, and sixteen Electrical Resistivity Tomography (ERT) profiles with lengths of 200 m and 400 m, achieving investigation depths of approximately 40 m and 80 m, respectively, using a gradient array. This approach enabled the acquisition of one and two-dimensional electrical resistivity profiles, allowing the

determination of material thicknesses, the identification of saturated zones, and the interpretation of geological structures.

2.1.3 Phase III: GIS-based mapping

Based on information obtained during the initial phases, cartographic inputs for the analysis of unstable area zoning were generated using Geographic Information System (GIS) tools.

The map of lithological units and structural lineaments was generated based on field-identified outcrops, analysis of lithological logs, interpretation of VES and ERT data, and photointerpretation of the Digital Elevation Model (DEM) and orthophotography (MAGAP).

The electrical resistivity map was developed by correlating values from VES and ERT surveys with the dominant stratigraphic units. A spatial interpolation process using the Inverse Distance Weighting (IDW) method was applied within a GIS environment to uniformly represent surface isoresistivity values, reflecting the distribution of materials and saturated zones [25].

Based on the DEM, a slope map was generated, with slope intervals defined in degrees using the GIS natural classification method, and aspect angles determined in azimuth degrees ranging from 0° to 360° relative to geographic north [26]. In addition, terrain concavity and convexity were derived with respect to the direction of maximum slope to identify zones of flow concentration and dispersion [27].

A supervised classification was implemented in a GIS environment using spectral signatures derived from orthophotography, following the guidelines proposed by Anderson et al. [28], to determine land use. Additionally, the drainage network's zones of influence were delineated using the GIS buffer tool, establishing spatial intervals that represent the relationship between fluvial dynamics and erosive processes. Likewise, IDW interpolation was applied to

rainfall data from CELEC EP at the Guarumales camp to represent the spatial distribution of precipitation.

2.1.4 Phase IV: Zoning of unstable areas

Susceptibility analysis was generated by rasterization thematic cartography at a 0.5 m/pixel spatial resolution in a GIS environment. Homogeneous categories were defined based on the reclassification of value ranges, supported by bibliographic references and knowledge of the sector-specific variables, as summarized in Table 1. Zoning was obtained through map algebra within a GIS environment by applying a weighted overlay of the normalized raster layers. The selection of the criteria used is based on the methodology proposed by Mora and Vahrson [23], which defines five essential factors for evaluating landslide susceptibility: slope, lithology, soil moisture, seismic intensity, and rainfall intensity. Furthermore, the weights assigned to each variable were defined using a heuristic approach, as described by Reichenbach et al. [24], which allowed the classification of susceptibility categories, resulting in the Eq. (2.1).

$$\text{Zoning} = 0.15 \cdot \text{L} + 0.15 \cdot \text{R} + 0.20 \cdot \text{P} + 0.15 \cdot \text{O} + 0.10 \cdot \text{C} + 0.1 \cdot \text{U} + 0.05 \cdot \text{D} + 0.1 \cdot \text{Q} \quad (2.1)$$

Where:

L: Lithology

R: Electrical resistivity

P: Slope

O: Orientation

C: Curvature

U: Land use

D: Distance to river

Q: Precipitation

Table 1

Variables and weightings for the reclassification of unstable area zoning

Parameters and references	**Susceptibility**				**Weighting**
	1 (Low)	**2 (Medium)**	**3 (High)**	**4 (Very high)**	
(1) Lithology	Andesite	Schists (sericitic, chloritic and quartzose)	Graphitic schist, alluvial	Active colluvium, colluvial-alluvial	0.15
(2) Resistivity [13]	> 5000 Ω·m	2000–4000 Ω·m	150–2000 Ω·m	< 75 Ω·m Saturated zones	0.15
(3) Slope [29], [30]	0°–15°	16°–30°	31°–50°	> 50°	0.2
(4) Orientation [29], [31]	Nort (NW315º–NE45º)	South (SE135º–SW225º)	East (NE45º–SE135º)	West (SW225º–NW315º)	0.1
(5) Curvature [32], [33]	Negative values		Positive values		0.1
(6) Land use [29], [33]	Urban fabric	Dense forest	Shrubland	Water bodies	0.1
(7) Distance to river [33], [34]	> 150 m	50–100 m	25–50 m	< 25 m	0.05
(8) Precipitation [35], [36]	< 125 mm	–250 mm	> 250 mm		0.15

Chapter 3

3.1 Results

3.1.1 Geoelectrical methods applied to unstable zones

A total of 16 ERTs and 6 VESs were conducted throughout the Guarumales camp (Figure 3). In the southern sector of the camp, where ERT-12, ERT-13, ERT-14, ERT-15, and ERT-16 were carried out, horizons with resistivities below 200 Ω·m were observed, extending from the surface to approximately 10 m depth (Figure 4). At greater depths (>30 m), low resistivities ranging from 400 to 1000 Ω·m were identified, suggesting the presence of colluvial or residual soils, or highly weathered rock.

Figure 3

Location of the geophysical survey

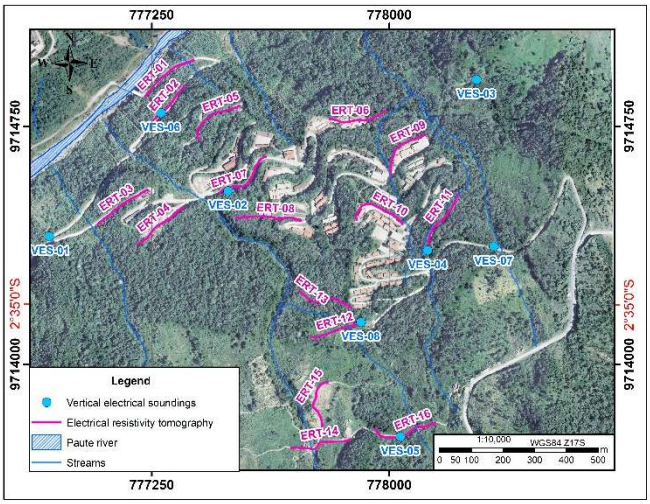

VES-05 shows conductive intervals ranging from 4 to 100 m (Figure 5), with resistivities below 100 Ω·m, suggesting that the southwestern area at elevation 1855 m is consistent with a water recharge environment. Resistivities below 150 Ω·m indicate the presence of saturated material, according to the classification presented in Table 2 of Alonso et al. [13].

Table 2

Relationship between resistivity and lithological material

Lithology	Resistivity range (Ω·m)
Saturated zones	< 75
Clayey material	75—175
Colluvial soil, residual soil, and highly weathered rock	175—1250
Colluvial	1250—3000
Weathered rock	3000—7000
Metavolcanic material / Igneous block	7000—9000
Fresh rock	>9000

In the intermediate slope area near the dining zone, at the camp elevation of 1580 m, the geoelectric profiles ERT-06 to ERT-10 (Figure 3) show localized saturation zones down to approximately 10 m depth (Figure 4). High resistivities are observed at the surface, associated with rock blocks within a colluvial matrix, while at depths where resistivities exceed 10,000 Ω·m, a continuous pattern along the survey suggests the presence of rock mass.

Conversely, in the northern part of the camp, near the Paute river channel at the lower slope, the geoelectric profiles ERT-01, ERT-02, and ERT-05 (Figure 3) indicate saturation zones in fine-grained materials down to approximately 10 m, while VES-06 also shows saturation of these materials starting at 30 m depth (Figure 5). This suggests that the area functions as a groundwater discharge zone, consistent with its topographic position within the camp. Being at the lowest point, subsurface flow from upper areas tends to converge there, promoting moisture

accumulation. Taken together, these geomorphological and hydrological conditions indicate that the observed saturations reflect the functioning of the local drainage system, where flow converges and discharges toward the base level. Table 2 summarizes the correlation between resistivity values and possible lithological types.

Figure 4

Schematic location of the geophysical survey campaign

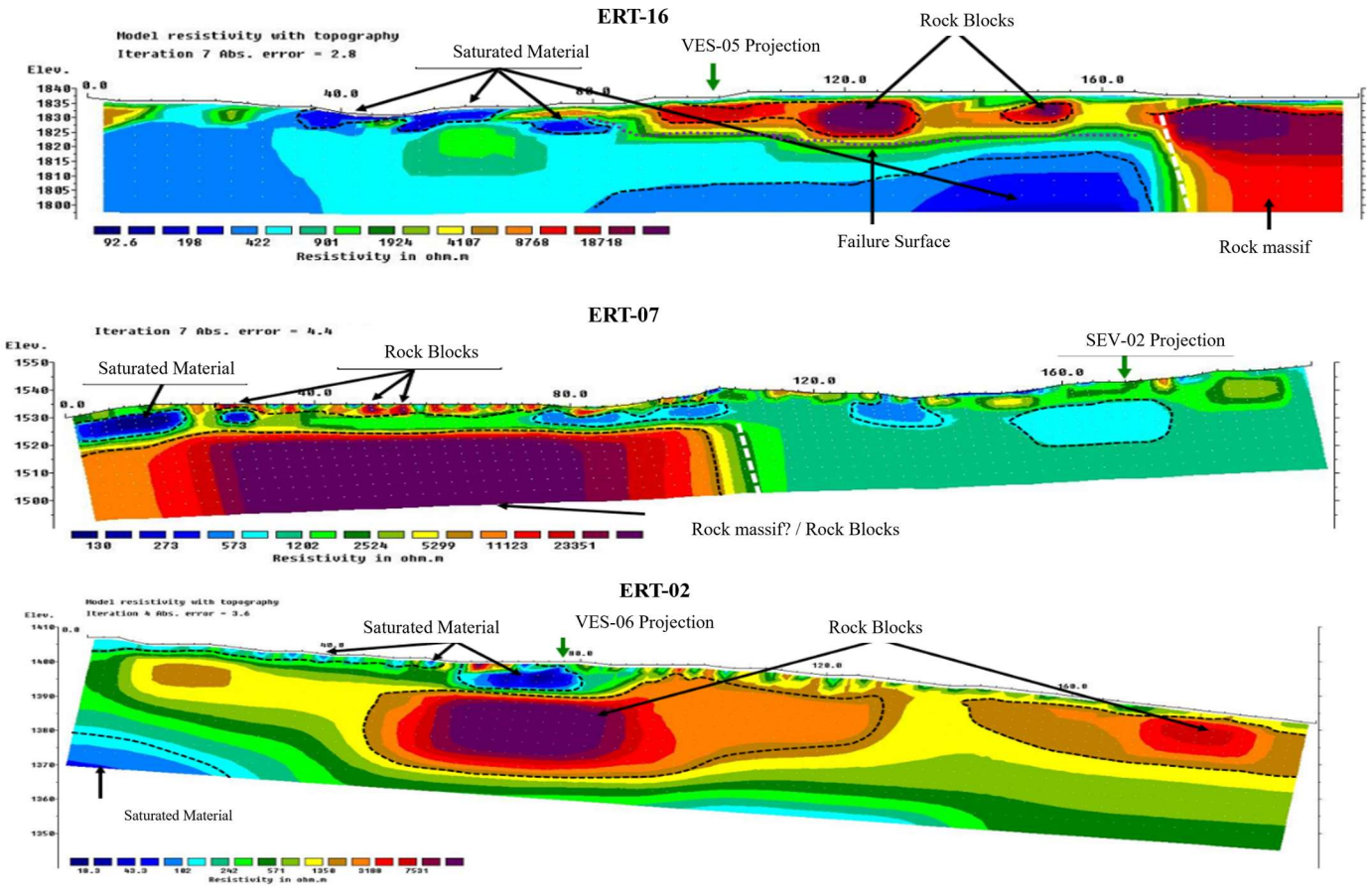

Figure 5

Representative VES geoelectrical profiles

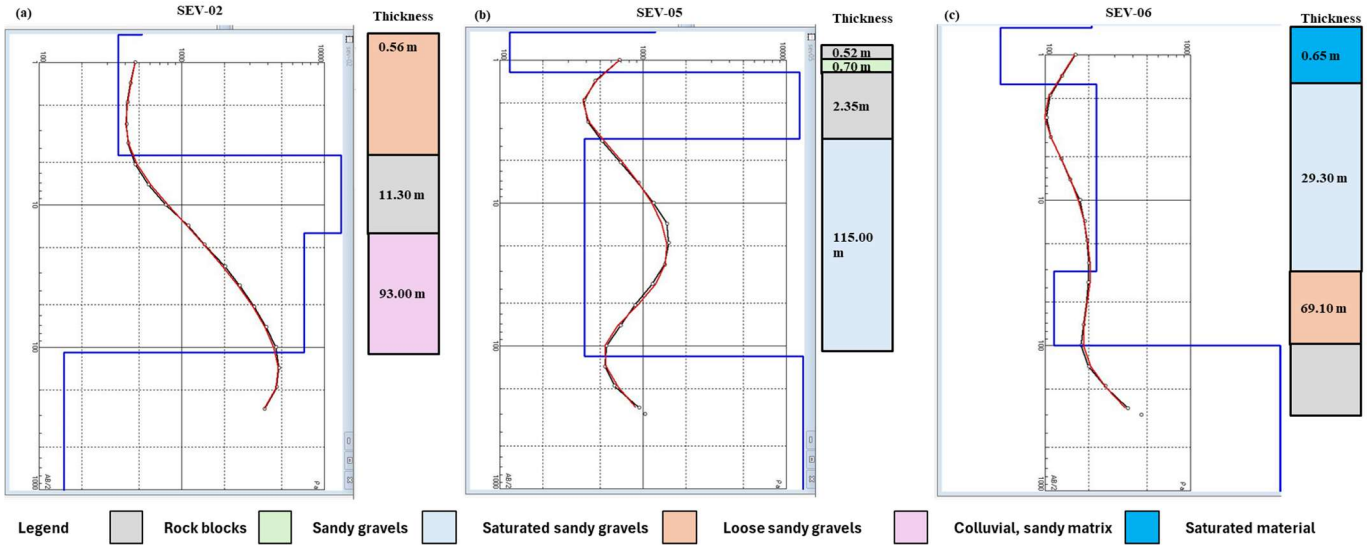

3.1.2 Application of GIS in analyzed variables

Based on the correlation between ERT and VES data with identified outcrops and historical boreholes, a basement composed of schists was determined at shallow depth in the northern part of the camp, whereas andesitic rocks are present at the surface in the eastern sector. Both lithological units are overlain by a thick colluvial deposit that, according to historical boreholes (PP-4) and geoelectric profiles, can reach up to 90 m in thickness in the southern part of the camp. Additionally, structural lineaments inferred from resistivity contrasts are delineated, and may be associated with basement, as shown in Figure 6.

Figure 6

Lithological units and structural lineaments

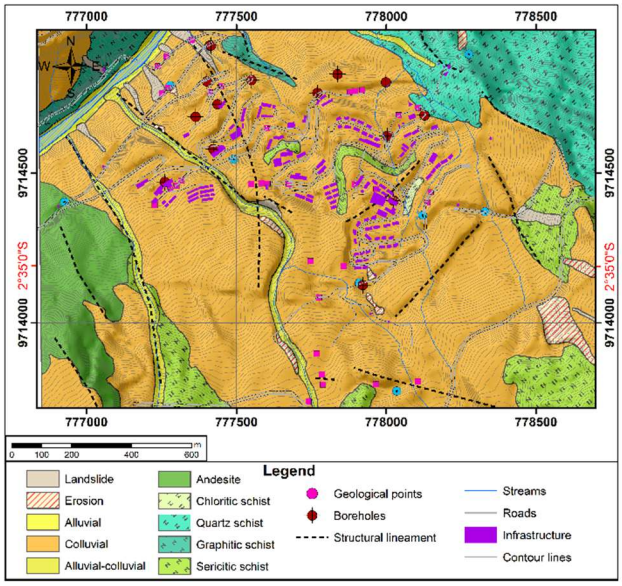

The isoresistivities in the intermediate and lower slope areas range from 19 to 200 Ω·m; these values suggest water saturation and low-competence materials, which, based on the geoelectric profiles, are interpreted as near-surface saturations down to 10 m depth. This could indicate the presence of springs or highly saturated zones, such as wetlands, consistent with site conditions. Conversely, historical boreholes (PP-1, PI-1) record more than 60 m of colluvial thickness in the lower slope area. In contrast, resistivity values approaching 10,000 Ω·m were obtained in the southern and western parts of the area, corresponding to fresh rock and large clasts, conditions that reduce the likelihood of instability in zones such as the intake point, treatment plant, and potable water reservoir located in the upper part of the camp (Figure 7).

Figure 7

Surface distribution of isoresistivity contours

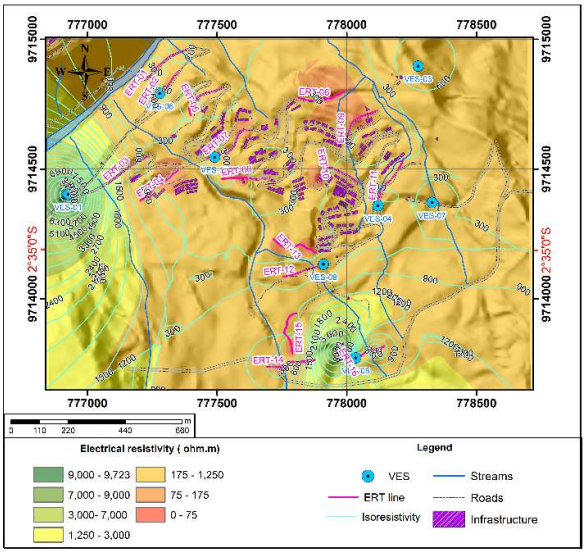

The morphology of the area corresponds to a mountainous relief with pronounced topographic variations, featuring slopes exceeding 53° along drainage channels and steep hillslopes with gradients greater than 60° in interfluvial zones, as shown in Figure 8.

Figure 8

Representation of terrain slopes

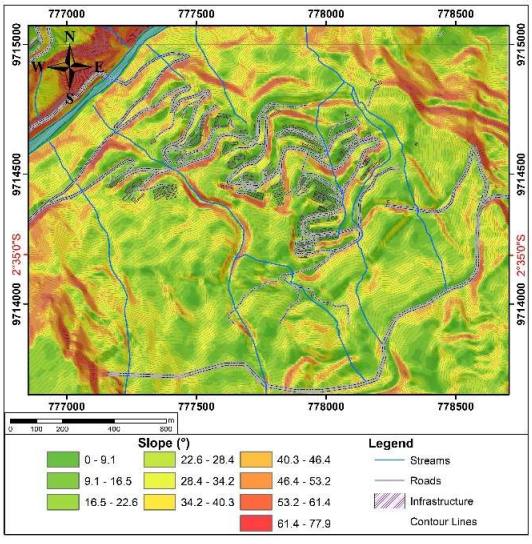

These morphologies, the drainage network, and poorly consolidated materials increase susceptibility to slope instability, with a higher incidence in the western and northwestern areas of the camp. In the study area, north-facing slopes dominate, with a smaller proportion facing south.

The alignment of the slopes in a similar direction to the overall slope gradient (toward the west) creates unfavorable conditions and increases the likelihood of instability processes (Figure 9).

Figure 9

Orientation relative to geographic north

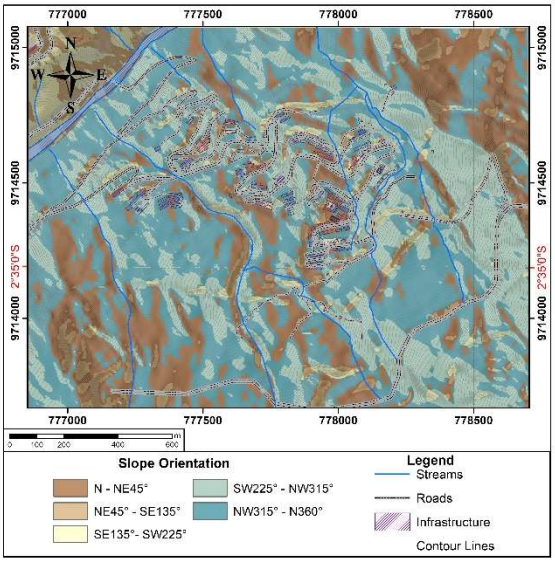

The morphologies of the study area are characterized by concave curvatures, represented by negative values, associated with flow accumulation and promoting increased erosion and instability, and convex curvatures, represented by positive values, corresponding to ridges and watersheds, which exhibit greater stability, although with potential for local failures. Flat curvature zones, represented by values close to zero and predominant in the central sector, correspond to transition surfaces between concave and convex curvature, or vice versa, where instability depends

on lithology and saturation degree (Figure 10). If the curvature transition zone is exceeded, subsidence or tension cracks may occur at these inflection points, serving as morphological indicators of instability zones.

Figure 10

Representation of terrain curvature

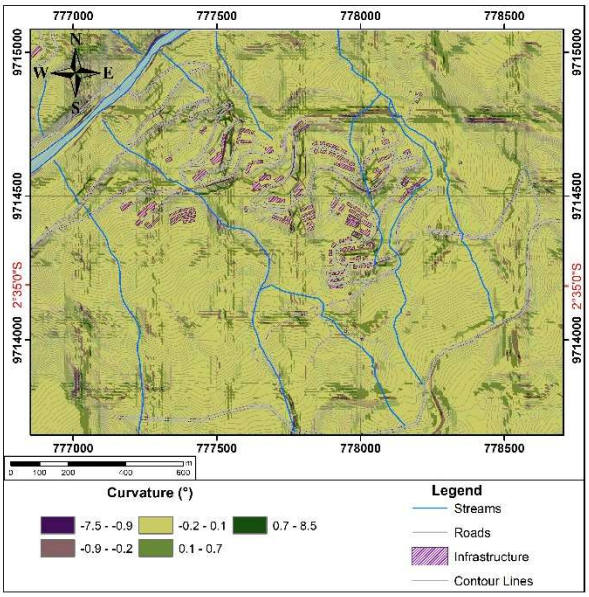

In the study area, 64% is dense forest, mainly covering the western and eastern parts of the camp. Approximately 28% of the area is covered by shrubland, which, while contributing to erosion reduction, also promotes water accumulation and the formation of groundwater recharge zones, mainly in the southern part of the camp. Urban fabric and water bodies account for 7.8% and 0.2% of the area, respectively, and are susceptible to erosion processes, particularly on steep slopes (Figure 11).

Figure 11

Representation of land use in the Guarumales camp

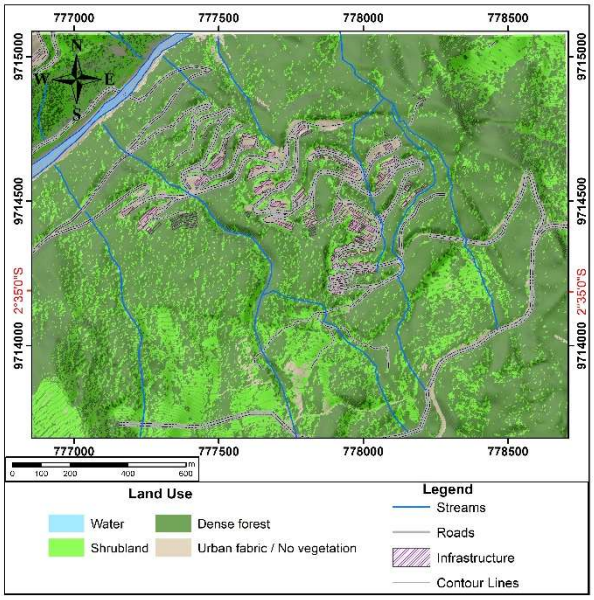

Water bodies, rivers, and streams contribute to erosion and undercutting on slopes; areas within 0 to 25 m of drainage channels exhibit higher susceptibility to erosion (Figure 12) due to direct water flow and lateral undercutting. In this context, the eastern and western sectors of the camp could be affected by these natural phenomena. The influence of fluvial dynamics, although less intense, can extend up to 50 m from the channel. Furthermore, areas located more than 50 m away show lower direct erosive impact from the drainage channels.

The study area experiences average monthly rainfall exceeding 250 mm/month (during the rainy season), which constitutes a critical factor for slope stability, as it intensifies water recharge in the upper slope, promotes saturation of poorly consolidated colluvial materials, and increases flow in the drainage network, enhancing erosion of slopes adjacent to the camp (Figure 13).

Figure 12

Distance ranges relative to the drainage network

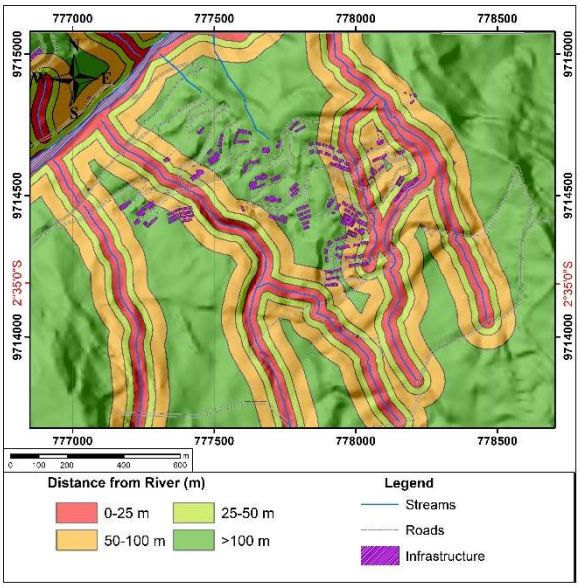

Figure 13

Isohyets and average monthly precipitation

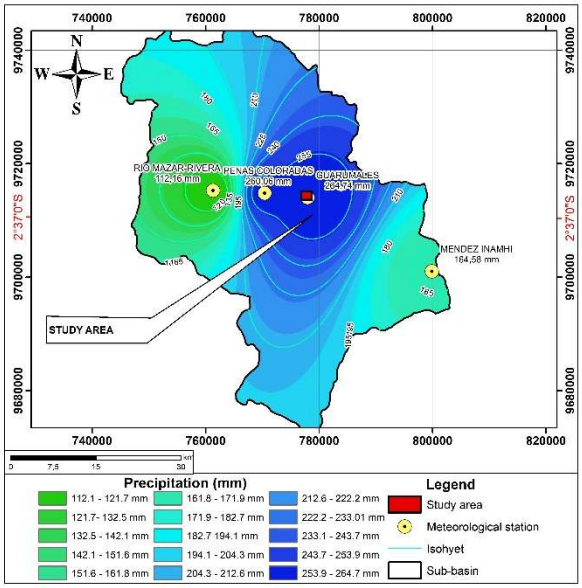

3.1.3 Mapping of unstable zones

Based on the mapping of unstable zones (see Figure 14), it was found that 5.60% of the area delineated as a macro-landslide by Robles Jéssica [9], exhibits moderately high to high susceptibility to FMR, 25.20% of the area shows moderate susceptibility, and 69.20% of the area is classified as very low to low.

The mapping (Figure 14) indicates higher susceptibility to mass movements along streams in the western and eastern parts of the camp, where erosion and lateral slope undercutting are evident. The occurrence of these processes coincides with areas closest to springs or drainage channels (<50 m; Figure 12), a condition classified as high to very high susceptibility (see Table 1), putting infrastructure located within a 50-meter radius of the streams at risk.

Likewise, as shown in Figure 14, the sector located in the northwestern part of the camp, south of the Paute river, exhibits moderate to high susceptibility. This occurrence is directly correlated with material saturation and the low consolidation of colluvial deposits, as analyzed through the isoresistivity mapping (Figure 7), thereby putting the existing road infrastructure at risk.

The southeastern sector of the study area exhibits moderate to moderately high susceptibility, with mass movements associated with the low consolidation of colluvial deposits, compromising road infrastructure. The camp area shows a moderate degree of susceptibility, related to sparse vegetation cover and steep slope gradients in the sector. Additionally, stream influence generates material saturation and erosion at the base of the slopes. The sector northwest of the Paute river exhibits moderate instability. This occurrence is directly associated with abrupt morphologies; although no slope failures are currently evident, erosion processes that could affect

this slope cannot be ruled out. In the 2012–2013 orthophotograph, erosion processes are observed at the upper part of the slope, which is composed of the colluvial deposit.

Figure 14

Mapping of unstable areas in the Guarumales camp

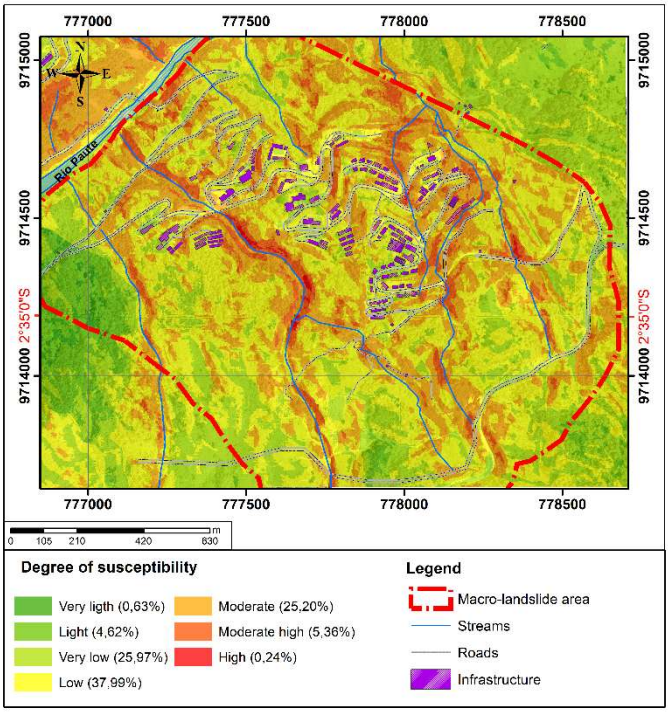

Chapter 4

4.1 Discussion

The landslide susceptibility map obtained in this study is based on the integration of multiple criteria: geophysical, geological, morphological, and hydrological.

Firstly, the interpretation of the geoelectric profiles revealed a strong correlation between low resistivity (<150 Ω·m) and the presence of saturated, low competence colluvial materials. This finding is consistent with the observations of Urgilez Vinueza et al. [8], who associated these values with areas of high landslide susceptibility in the Paute Integral hydroelectric complex. However, it is important to consider that the spatial variation in ERT isoresistivities can be influenced by heterogeneity in the deposits, introducing uncertainties in the precise delineation of layers.

Regarding the weights assigned in the multi-criteria weighting, although these are based on heuristic approaches validated in the scientific literature [21], their application involves a certain degree of subjectivity.

From a hydrological perspective, a clear relationship was identified between proximity to drainage channels (<50 m), steep slopes (>53°), and low resistivity values, suggesting a synergy between saturation, surface runoff, and fluvial erosion, as reported by Vire [15]. However, the spatial interpolation of precipitation may introduce uncertainty due to the low density of meteorological stations in mountainous areas such as Guarumales. Increasing the number of stations or integrating regional climate models would allow a more accurate representation of the rainfall regime, improving the estimation of triggering factors for instability.

From a geomorphological perspective, concave curvatures and steep slopes favor moisture accumulation, creating conditions conducive to instability. However, the current model does not incorporate temporal variations of the water table, which represents a limitation, particularly

during extreme rainfall events—those exceeding the 95th–99th percentile or exhibiting high intensities over short periods—capable of rapidly saturating the terrain, as observed in analyses of extreme rainfall events in the southern Andes of Ecuador [37]. Previous studies, such as Alonso-Pandavenes et al. [13] highlight the importance of integrating transient groundwater flow analyses to understand the dynamic evolution of these processes.

Although the susceptibility mapping (Figure 14) shows spatial coherence with the observed field processes and constitutes a relevant technical tool for risk management, it is important to consider that susceptibility levels may vary over short time periods. For example, areas classified as moderately susceptible, such as the northeastern sector of the camp, could experience significant instability during seasonal saturation events or anthropogenic activities (construction or deforestation). Conversely, areas categorized as stable (very low to low susceptibility), such as most of the residential, casino, and dining areas, could degrade due to changes in land use. Therefore, the mapping should be interpreted as a dynamic input, that can be updated. These factors reinforce the need to maintain a permanent monitoring system, such as the one currently implemented by CELEC EP [8], which should focus on sectors designated as moderately high and high in susceptibility to refine evaluations and continuously update the mapping.

To evaluate the consistency of the results obtained in the susceptibility mapping, the resistivity profile A–A' (Figure 15) was generated, crossing the northern sector of the camp from the upper slope in the east to the lower slope in the west. This profile allows analysis of the relationship between the resistivity distribution, geomorphological conditions, and the susceptibility levels identified in the mapping.

Figure 15

Section A-A' crossing the northern sector of the camp from the upper slope in the east to the lower slope in the west

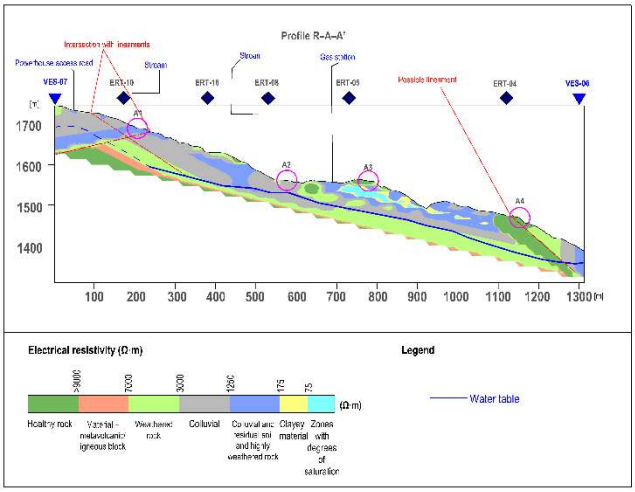

Four points of interest are identified along with this profile, as shown in Figure 16. At point A1, located in the northeastern sector of the camp and corresponding to the beginning of the profile, residual strata and weathered rock outcrop at the surface, followed by a layer of colluvial material. With increasing depth, resistivity values increase, reflecting the transition from weathered rock to igneous rock, and, finally, to fresh rock. This behavior is consistent with the moderate susceptibility level determined for the sector, attributable to the superficial presence of colluvial and residual materials, which exhibit a high propensity for landslide activity under steep slope conditions.

Figure 16

Section location in plan view

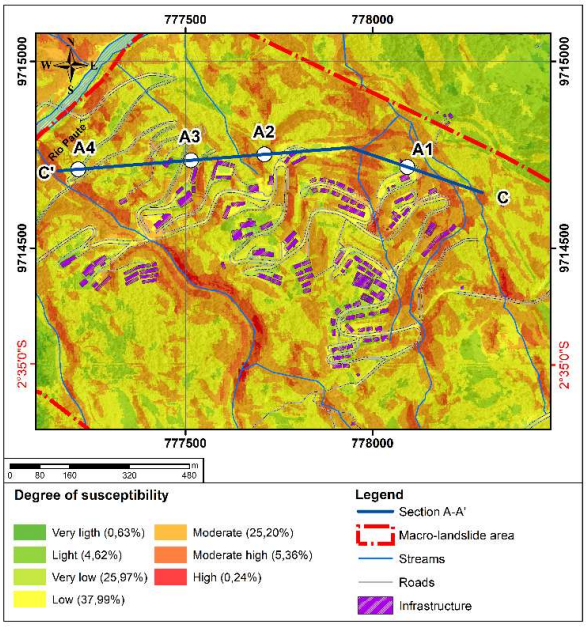

Point A2, located approximately 600 m from the beginning of profile A–A', is characterized by the presence of thick colluvial deposits overlying a layer of weathered rock. Compared to susceptibility map, this sector corresponds to an area with low to moderate susceptibility. Despite intermediate resistivity values, instability is limited by gentle slopes and the progressively decreasing influence of fluvial processes with increasing distance from the stream.

Point A3, located approximately 800 m from the beginning of the profile, exhibits at the surface a layer of weathered rock interbedded with colluvial material. At greater depth, a marked decrease in resistivity values is observed, interpreted as the presence of highly saturated materials, possibly saturated clays, underlying thick colluvial deposits and weathered rock. According to the susceptibility mapping, this sector is classified as moderately high to high susceptibility. This configuration represents a scenario conducive to instability, as competent layers are identified at

the upper and lower levels. At the same time, the intermediate zone is dominated by lower-strength strata with high saturation, which could constitute a preferential sliding surface.

Finally, point A4, located approximately 1,200 m from the beginning of profile A–A' in the northwestern sector of the camp, is characterized by highly competent layers of fresh rock overlain by weathered rock. This stratigraphic condition is consistent with the susceptibility mapping, which classifies as low to very low susceptibility, in accordance with the high resistivity values and the relatively gentle slopes of the sector.

In general, the spatial correspondence between the mapping of unstable areas and the geoelectric profile A–A' shows a high internal consistency, supporting the applicability and robustness of the proposed methodology for similar studies in complex geological settings.

Finally, this multidisciplinary approach enabled a coherent representation of terrain conditions and their relative stability. However, the results also reveal limitations that need to be addressed to strengthen the method's scientific robustness of the method. The heterogeneity of colluvial deposits introduces uncertainty in delineating isoresistivities, underscoring the need to increase the density of ERT–VES profiles to better define transitional zones. Furthermore, the multi-criteria weighting used, although supported by specialized literature, retains a subjective component that could be refined using multivariate statistical methods or machine learning models to quantify each variable's actual weight. Similarly, the absence of direct geotechnical information (such as triaxial tests, permeability, unit weights, undrained and drained shear strength parameters) limits the validation of geoelectric interpretations. Incorporating these parameters would allow for a more precise correlation between resistivity ranges and the material's effective competence. Finally, future studies should integrate transient hydrogeological monitoring (water table levels and pore pressures) to capture the effects of extreme events, thereby strengthening the

conceptual framework underpinning this scientific and technical contribution. A total of 915,936 m^3 is classified as areas of moderately high to high susceptibility to landslides.

Chapter 5

5.1 Conclusions

The integration of geological, geomorphological, hydro-meteorological, and geoelectric information enabled precise characterization of the physical conditions controlling instability at the Guarumales camp. This is due to the combination of fractured schists, thick colluvial deposits, and high moisture levels, which create an environment highly susceptible to mass removal phenomena (MRP). Steep slopes (>53°), concave curvatures, proximity to drainage channels (0–25 m), and rainfall exceeding 250 mm/month (seasonal rainy period, three months) are key conditioning and triggering factors, that intensify saturation and the loss of material strength.

During this research, electrical resistivity proved to be a critical parameter for discriminating between saturation domains and material competence. Resistivity values below 175 Ω·m were associated with fragile, saturated materials, while values above 3,000 Ω·m indicated more competent, stable conditions.

The correlation between ERT and VES methods, together with geomorphological factors, enabled the generation of a spatial map of landslide susceptibility, clearly identifying areas of highest priority for risk management. The areas of greatest interest are those classified as high, moderately high, and moderate susceptibility, accounting for 0.24%, 5.36%, and 25.20% of the area delineated as the macro-landslide zone, respectively. This study provides a methodological baseline for stability assessment in complex, mountainous terrain with similar characteristics, using combined geophysical methods.

The susceptibility mapping shows that high-susceptibility areas are concentrated along drainage channels and their margins, forming critical corridors that increase exposure of roads and infrastructure points. Although most buildings are in low-susceptibility zones, the influence of high-susceptibility strips highlights the need for continuous preventive management.

In terms of risk management and mitigation, the results of this study provide a technical input for mapping sectors that require optimization and reinforcement, and for identifying areas where erosion control and drainage improvements would be most effective, such as the north-northwestern sector of the camp, which exhibits the highest susceptibility. Additionally, the saturated domains identified through geoelectric surveys facilitate the design of engineering solutions, such as deep horizontal drains, lined channels, slope reconfiguration, or revegetation on low-competence slopes.

The results show strong agreement between the susceptibility mapping, geoelectric profiles, and the geomorphological conditions observed in the field, with spatial correspondence between low-resistivity domains, steep slopes, and proximity to drainage channels reinforcing the internal consistency of the analysis and the interpretation of the conditioning factors of instability. This supports the robustness of the adopted methodological approach and the reliability of the mapping as a tool for risk assessment and management in the Guarumales camp. To strengthen this methodological contribution and expand its applicability, future research should incorporate geotechnical parameters that allow quantitative correlation of resistivity ranges with the mechanical properties of soil and rock, to validate and calibrate the identified geoelectric domains, as well as integrate seasonal monitoring (rainy and dry periods) of the water table. In this regard, the study provides a solid technical and scientific framework for assessing unstable slopes and reducing of risk in critical infrastructure, establishing methodological bases that can be replicated in other large-scale projects in mountainous areas of Ecuador and the Andean region.

Acknowledgment

The authors express their sincere gratitude to the Master's Program in Geotechnics (FICT-ESPOL) for the academic training provided and its commitment to educational excellence. The CIPAT-ESPOL research center contributed technical personnel, logistical support, and geophysical equipment necessary for the field investigations. The authors also acknowledge CELEC EP for the facilities provided and for granting access to relevant information that made the development of this research possible.

References

[1] Pourghasemi, H. R., Pouyan, S., Bordbar, M., Golkar, F., & Clague, J. J. (2023). Flood, landslides, forest fire, and earthquake susceptibility maps using machine learning techniques and their combination. *Natural Hazards*, *116*(3), 3797–3816. https://doi.org/10.1007/s11069-023-05836-y

[2] Dai, F. C., Lee, C. F., & Ngai, Y. Y. (2002). Landslide risk assessment and management: an overview. *Engineering Geology*, *64*(1), 65–87. https://doi.org/10.1016/S0013-7952(01)00093-X

[3] Regmi, S., & Dahal, R. K. (2024). Consequences of slope instability and existing practices of mitigation in hydropower projects of Nepal. *Geoenvironmental Disasters*, *11*(1), 26. https://doi.org/10.1186/s40677-024-00289-2

[4] Mirzaei, V., Abadi, M., Mirhabibi, M., Mohammad Bagher, A., Vahid, M., Mohsen, M., Parvin, D., Bagher, A. M., & Dehghani, P. (2015). Hydroelectric Energy Advantages and Disadvantages. In *Hydroelectric Energy Advantages and Disadvantages. American Journal of Energy Science* (Vol. 2, Issue 2). http://www.openscienceonline.com/journal/energy

[5] Dogan, M., Sahin, S., Ullah, A., & Safi, A. (2024). Promoting environmental sustainability: A policy perspective on hydroelectric power generation, foreign direct investments, and financial development. *Energy*, *312*, 133576. https://doi.org/10.1016/J.ENERGY.2024.133576

[6] CELEC EP. (2024). *Plan Estratégico Empresarial 2024 - 2025.*

[7] Agencia de Regulación y Control de Electricidad. (2025). *Panorama Eléctrico*. https://arconel.gob.ec/wp-content/uploads/downloads/2025/05/Revista28-versionGobierno-v5.pdf

[8] Urgilez Vinueza, A., Robles, J., Bakker, M., Guzman, P., & Bogaard, T. (2020). *Characterization and Hydrological Analysis of the Guarumales Deep-Seated Landslide in the Tropical Ecuadorian Andes*. https://doi.org/https://doi.org/10.3390/geosciences10070267

[9] Robles Jéssica. (2020). *Caracterización y microzonificación del Macro deslizamiento Guarumales y propuesta de medidas de mitigación, Azuay-Ecuador*.

[10] El Universo. (2020, June 2). Aluvión bloquea el paso entre Azuay y Morona Santiago. *Https://Www.Eluniverso.Com/Noticias/2020/06/02/Nota/7859286/Deslizamiento-Amaluza-Sevilla-Oro-Azuay/*.

[11] La Hora. (2002, July 17). Las tragedias en el Oriente no paran. *Https://Www.Lahora.Com.Ec/Noticias/Las-Tragedias-En-El-Oriente-No-Paran/*.

[12] Corporación Eléctrica del Ecuador. (2020, October 23). *CELEC EP financia la construcción del puente sobre la quebrada Jurupis, sector Amaluza, en Azuay*. Https://Www.Celec.Gob.Ec/Hidroagoyan/Noticias-Noticias/Celec-Ep-y-El-Mtop-Construiran-Nuevo-Puente-Sobre-La-Quebrada-Jurupis-Sector-Amaluza/.

[13] Alonso-Pandavenes, O., Torrijo, F. J., Garzón-Roca, J., & Gracia, A. (2023). Early Investigation of a Landslide Sliding Surface by HVSR and VES Geophysical Techniques Combined, a Case Study in Guarumales (Ecuador). *Applied Sciences (Switzerland)*, *13*(2). https://doi.org/10.3390/app13021023

[14] Carrión-Mero, P., Tiviano, I., Hervas, E., Jaya-Montalvo, M., Malavé-Hernández, J., Solórzano, J., Berrezueta, E., & Morante-Carballo, F. (2023). Water Sowing and harvesting application for water management on the slopes of a volcano. *Heliyon*, *9*(5), e16029. https://doi.org/10.1016/J.HELIYON.2023.E16029

[15] Vire Camila. (2024). *Prospección geofísica en los movimientos en masa aguas arriba de la represa del Delsitanisagua, provincia de Zamora Chinchipe.* Universidad Nacional de Loja.

[16] Macías, L., Quiñonez-Macías, M., Toulkeridis, T., & Pastor, J. L. (2024). Characterization and geophysical evaluation of the recent 2023 Alausí landslide in the northern Andes of Ecuador. *Landslides*, *21*(3), 529–540. https://doi.org/10.1007/s10346-023-02185-6

[17] Solórzano, J., Morante-Carballo, F., Montalván-Burbano, N., Briones-Bitar, J., & Carrión-Mero, P. (2022). A Systematic Review of the Relationship between Geotechnics and Disasters. *Sustainability*, *14*(19), 12835. https://doi.org/10.3390/su141912835

[18] Varnes David J. (1984). *Landslide hazard zonation: a review of principles and practice (No. 3).*

[19] Bravo-López, E., Fernández Del Castillo, T., Sellers, C., & Delgado-García, J. (2023). Analysis of Conditioning Factors in Cuenca, Ecuador, for Landslide Susceptibility Maps Generation Employing Machine Learning Methods. *Land*, *12*(6). https://doi.org/10.3390/land12061135

[20] Carrión-Mero, P., Solórzano, J., Malavé-Hernández, J., Martínez-Angulo, J., Javier, M. F., & Morante-Carballo, F. (2024). Mapping Groundwater Potential Zones for Sustainable Agricultural Development in Entre Ríos, Ecuador. *International Journal of Design & Nature and Ecodynamics*, *19*(3), 817–830. https://doi.org/10.18280/ijdne.190312

[21] Torrijo, F. J., Álvarez, S., & Garzón-Roca, J. (2024). A Case Study of a Macro-Landslide in the High Mountain Areas of the Ecuadorian Andes: “La Cría” at the Azuay Province (Ecuador). *Land*, *13*(12). https://doi.org/10.3390/land13122047

[22] Carrión-Mero, P., Dueñas-Tovar, J., Jaya-Montalvo, M., Berrezueta, E., & Jiménez-Orellana, N. (2022). Geodiversity assessment to regional scale: Ecuador as a case study. *Environmental Science & Policy*, *136*, 167–186. https://doi.org/10.1016/J.ENVSCI.2022.06.009

[23] Mora C., S., & Vahrson, W.-G. (1994). Macrozonation Methodology for Landslide Hazard Determination. *Environmental & Engineering Geoscience*, *xxxi*(1), 49–58. https://doi.org/10.2113/gseegeosci.xxxi.1.49

[24] Reichenbach, P., Rossi, M., Malamud, B. D., Mihir, M., & Guzzetti, F. (2018). A review of statistically-based landslide susceptibility models. *Earth-Science Reviews*, *180*, 60–91. https://doi.org/10.1016/j.earscirev.2018.03.001

[25] El Makrini, S., Boualoul, M., Mamouch, Y., El Makrini, H., Allaoui, A., Randazzo, G., Roubil, A., El Hafyani, M., Lanza, S., & Muzirafuti, A. (2022). Vertical Electrical Sounding (VES) Technique to Map Potential Aquifers of the Guigou Plain (Middle Atlas, Morocco): Hydrogeological Implications. *Applied Sciences*, *12*(24), 12829. https://doi.org/10.3390/app122412829

[26] Wilson John P., & Gallant John C. (2000). *Terrain Analysis Principles and Applications*.

[27] Buckley, A. (2010). *Understanding curvature rasters*. Blog de ESRI.

[28] Anderson, J. R., Hardy, E. E., Roach, J. T., & Witmer, R. E. (1976). *A Land Use and Land Cover Classification System for Use with Remote Sensor Data*.

[29] Fernandez-Lavado, C. (2008). *Manual metodológico para la evaluación de movimientos de ladera en el AMSS (El Salvador, CA)*.

[30] Foumelis, M., Lekkas, E., & Parcharidis, I. (2018). Landslide susceptibility mapping by GIS-Based Qualitative weighting procedure in Corinth area. *Bulletin of the Geological Society of Greece*, *36*(2), 904. https://doi.org/10.12681/bgsg.16840

[31] Ponce de León, D., San Antonio, J., Mañe Jane, R., & Seisdedos Santos, J. (2003). *Caracterización de los riesgos geológicos y dimensionamiento de los recursos hidrogeológicos. Directrices para la ordenación territorial del municipio de Nejapa.*

[32] Xu, K., Zhao, Z., Chen, W., Ma, J., Liu, F., Zhang, Y., & Ren, Z. (2024). Comparative study on landslide susceptibility mapping based on different ratios of training samples and testing samples by using RF and FR-RF models. *Natural Hazards Research*, *4*(1), 62–74. https://doi.org/10.1016/j.nhres.2023.07.004

[33] Cobin, P. F. (2013). *Probabilistic modeling of rainfall induced landslide hazard assessment in San Juan Lla Laguna, Sololá, Guatemala* [Michigan Technological University]. https://doi.org/10.37099/mtu.dc.etds/700

[34] Kıncal, C., Li, Z., Drummond, J., Liu, P., Hoey, T., & Muller, J.-P. (2017). Landslide Susceptibility Mapping Using GIS-based Vector Grid File (VGF) Validating with InSAR Techniques: Three Gorges, Yangtze River (China). *AIMS Geosciences*, *3*(1), 116–141. https://doi.org/10.3934/geosci.2017.1.116

[35] Quesada Román, A., & Feoli Boraschi, S. (2018). Comparación de la Metodología Mora-Vahrson y el Método Morfométrico para Determinar Áreas Susceptibles a Deslizamientos en la Microcuenca del Río Macho, Costa Rica. *Revista Geográfica de América Central*, *1*(60). https://doi.org/10.15359/rgac.61-2.1

[36] Chacón, J., Irigaray, C., Fernández, T., & El Hamdouni, R. (2006). Engineering geology maps: landslides and geographical information systems. *Bulletin of Engineering Geology and the Environment*, *65*(4), 341–411. https://doi.org/10.1007/s10064-006-0064-z

[37] Urgilés, G., Célleri, R., Bendix, J., & Orellana-Alvear, J. (2024). Identification of spatio-temporal patterns in extreme rainfall events in the Tropical Andes: A clustering analysis approach. *Meteorological Applications*, *31*(5). https://doi.org/10.1002/met.70005